

Unique features of structure in an odd-proton $N \approx Z$ nucleus ^{69}As

M. Hasegawa,¹ K. Kaneko,² and T. Mizusaki,³

¹Laboratory of Physics, Fukuoka Dental College, Fukuoka 814-0193, Japan

²Department of Physics, Kyushu Sangyo University, Fukuoka 813-8503, Japan

³Institute of Natural Sciences, Senshu University, Tokyo 101-8425, Japan

(Dated: September 8, 2018)

We apply a large-scale shell model to the study of proton-rich odd-mass nuclei with $N \approx Z$. Calculations predict unexpected structure in the ^{69}As nucleus for which a detailed experiment was recently performed. In this odd-proton nucleus, one neutron competes with one proton for occupying the high- j intruder orbit $g_{9/2}$ in the $9/2_1^+$ state and almost solely occupies the $g_{9/2}$ orbit in other low-lying positive-parity states. The $T = 0$, $J = 9$ one-proton-one-neutron alignment takes place in the negative-parity states with medium-high spins. A unique coexistence of two lowest bands with positive and negative signs of spectroscopic quadrupole moments is predicted.

PACS numbers: 21.60.Cs, 21.10.-k, 27.50.+e

I. INTRODUCTION

The study of $N \approx Z$ proton-rich nuclei with $A = 60 - 100$ is one of current topics in nuclear physics. These nuclei have provided plenty of phenomena exhibiting interesting structure such as rapid shape changes with increasing N , Z , and J (spin). Strong residual correlations between protons and neutrons which are inherent properties of nuclei play a key role in these $N \approx Z$ fp -shell nuclei. Experiments are extensively accumulating a variety of unique phenomena which demand theoretical explanations. The shape changes, shape coexistence, and particle alignments have been investigated intensively in even-even $N \approx Z$ nuclei until now (for instance, see latest work [1, 2, 3, 4, 5, 6, 7, 8, 9]), but they have not fully been discussed in odd-mass $N \approx Z$ nuclei and odd-odd $N \approx Z$ nuclei [10, 11]. One of the reasons apart from experimental difficulty is that theoretical approaches employed are not necessarily fit to describe these properties of odd-mass and odd-odd nuclei.

Recently, the spherical shell model has become capable of calculating $A = 60 - 70$ nuclei in the $pf_{5/2}g_{9/2}$ shell. The shell model calculations reproduce observed energy levels up to high spins in these nuclei and successfully explain shape changes from ^{64}Ge to ^{68}Se along the even-even $N = Z$ line and various particle alignments in even-even nuclei [12, 13, 14]. The shell model predicts unexpected alignment in this mass region. More precisely, $T = 0$ one-proton-one-neutron ($1p1n$) alignment in the high- j $g_{9/2}$ orbit takes place not only in odd-odd nuclei but also in even-even nuclei. In addition, the shell model calculation [15] revealed possible shape difference between low-lying states in the odd-odd $N = Z$ nucleus ^{66}As , predicting a shape isomer. These calculations suggest that unusual structure observed in even-even $N \approx Z$ nuclei would occur in odd-mass and odd-odd nuclei of this mass region and the reverse also could happen. A further study of the questions must contribute to elucidation of various features of nuclear structure.

In this paper, we are interested in the question what characteristics appear in odd-mass $N \approx Z$ nuclei. Our

previous paper [15], where the isomeric state $9/2_1^+$ in ^{67}As was investigated, found unique structure formed in the odd-proton $N \approx Z$ nucleus. A recent experiment carried out by Stefanescu *et al.* [16] has provided much new information in the nucleus ^{69}As as compared with nearby other odd-mass nuclei. Three doublets of negative- and positive-parity bands and high-spin states up to band terminations are observed in ^{69}As . The very detailed data seem to conceal unknown features of odd-proton fp -shell nuclei and are worth investigating. The shell model calculation which gives precise wave functions for yrast and non-yrast states is expected to be fruitful for the investigation.

II. THE MODEL

We employ the same shell model with the single-particle states ($p_{3/2}$, $f_{5/2}$, $p_{1/2}$, $g_{9/2}$) as that used for ^{66}As and ^{67}As in Ref. [15]. The extended $P+QQ$ Hamiltonian used here is composed of the single-particle energies, $T = 0$ monopole field ($H_{\pi\nu}^{T=0}$), monopole corrections (H_{mc}), $J = 0$ pairing force (H_{P_0}), quadrupole-quadrupole force (H_{QQ}) and octupole-octupole force (H_{OO}):

$$\begin{aligned} H &= H_{\text{sp}} + H_{\pi\nu}^{T=0} + H_{\text{mc}} + H_{P_0} + H_{QQ} + H_{OO} \\ &= \sum_{\alpha} \varepsilon_{\alpha} c_{\alpha}^{\dagger} c_{\alpha} - k^0 \sum_{a \leq b} \sum_{JM} A_{JM00}^{\dagger}(ab) A_{JM00}(ab) \\ &+ \sum_{a \leq b} \sum_T \Delta k_{\text{mc}}^T(ab) \sum_{JMK} A_{JMTK}^{\dagger}(ab) A_{JMTK}(ab) \\ &- \frac{1}{2} g_0 \sum_K P_{001K}^{\dagger} P_{001K} \\ &- \frac{1}{2} \frac{\chi_2}{b^4} \sum_M : Q_{2M}^{\dagger} Q_{2M} : - \frac{1}{2} \frac{\chi_3}{b^6} \sum_M : O_{3M}^{\dagger} O_{3M} : \end{aligned} \quad (1)$$

where $A_{JMTK}^{\dagger}(ab)$ is a pair creation operator with spin JM and isospin TK in the orbits (ab). This shell model has proven to be rather successful in describing $A = 64 - 70$ nuclei such as ^{65}Ge , ^{67}Ge , ^{66}As , ^{67}As , and neighboring

even-even nuclei up to ^{70}Ge . For more details, see Refs. [12, 13, 14, 15]. Some specifics are reviewed below.

We made a search for good parameters which describe even- and odd-mass Ge isotopes [14]. The single-particle energies of the four orbits are obtained as $\varepsilon_{p_{3/2}} = 0.0$, $\varepsilon_{f_{5/2}} = 0.77$, $\varepsilon_{p_{1/2}} = 1.11$, and $\varepsilon_{g_{9/2}} = 2.50$ in MeV. The value $\varepsilon_{g_{9/2}} = 2.5$ MeV differs from 3.7 MeV extracted from ^{57}Ni in Ref. [17] but coincides with that of Ref. [18]. It is difficult to reproduce the energy levels ($9/2^+$ and others) of the odd-mass Ge isotopes ^{65}Ge and ^{67}Ge unless we lower the energy $\varepsilon_{g_{9/2}}$ to 2.5 MeV. The monopole field $H_{\pi\nu}^{T=0}$, which depends only on the total isospin and the number of valence nucleons, does not affect excitation energies considered in this paper. Because the isospin is a good quantum number in $N \approx Z$ nuclei, we set the Hamiltonian to conserve the isospin. The parameter search gave the force strengths ($g_0 = 0.27(64/A)$, $\chi_2 = 0.25(64/A)^{5/3}$, and $\chi_3 = 0.05(64/A)^2$ in MeV) and five parameters of the monopole corrections. Three of the monopole corrections ($\Delta k_{\text{mc}}^{T=1}(p_{3/2}, f_{5/2}) = \Delta k_{\text{mc}}^{T=1}(p_{3/2}, p_{1/2}) = -0.3$ and $\Delta k_{\text{mc}}^{T=1}(f_{5/2}, p_{1/2}) = -0.4$ in MeV) are important for the collectivity in the $(p_{3/2}, f_{5/2}, p_{1/2})$ subspace. Especially, $\Delta k_{\text{mc}}^{T=1}(f_{5/2}, p_{1/2})$ plays an important role in producing the oblate shape for ^{68}Se and ^{72}Kr [13]. The study of isomeric states in ^{66}As and ^{67}As compelled us to make a modification to the monopole corrections [15]. The additional terms are $\Delta k_{\text{mc}}^{T=0}(a, g_{9/2}) = -0.18$ MeV ($a = p_{3/2}, f_{5/2}, p_{1/2}$). These corrections have an effect of lowering $\varepsilon_{g_{9/2}}$ further but the effect is different from wide effects caused by directly decreasing $\varepsilon_{g_{9/2}}$. Our calculations suggest that a special contribution of the $g_{9/2}$ orbit may be related to the rapid structure change when Z and N approaching 40, although the parameter-fitting treatment does not explain the physical origin.

In this paper, we carry out large-scale shell model calculations for ^{69}As using the code [19], which diagonalizes shell model Hamiltonian matrix in M -scheme. As, in M -scheme, shell model dimensions decrease as a function of $|M|$ value, lower spin state needs bigger shell model dimension and there is a case that higher spin states are easily solved while the lower spin states can not be solved exactly. In the present case, the low-spin states with $J^\pi \leq 7/2^-$ or $J^\pi \leq 9/2^+$ in ^{69}As have a dimension of the Hamiltonian matrix larger than 2×10^8 . The dimension exceeds the capacity of our personal computers. Therefore, we truncate the matrix by limiting the number t in the configuration space $\sum_{n \geq t} (p_{3/2}, f_{5/2})^n (p_{1/2}, g_{9/2})^{13-n}$. For $3/2^-$ states, for instance, the dimension is 1.996×10^8 when $t = 5$. For ^{69}As , however, the maximum dimension is at most 2.4×10^8 and hence the $t = 5$ truncation ($t = 2$ for $9/2^+$) is expected to be good enough for our discussions.

For more accurate calculations, we consider the energy variance extrapolation method [20], which can evaluate exact energy from the truncated wave functions based on the scaling property between energy difference δE

and energy variance ΔE , i.e., $\delta E \propto \Delta E$. Here we use a new formula of energy variance extrapolation derived by introducing a lowest energy projection operator \hat{R} to approximated wave function $|\varphi\rangle$. As $\hat{R}|\varphi\rangle$ is a better wave function, it gives more precise estimation. In fact, we use \sqrt{H} as \hat{R} and a new scaling relation can be derived, which involves the expectation value of H^3 [21]. In the case of ^{69}As , this extrapolation gives exact energies within the accuracy 1 keV. We have found that the results in the slightly truncated spaces for the states with $J^\pi \leq 7/2^-$ or $J^\pi \leq 9/2^+$ are almost exact. The extrapolation improves energies only by several keV.

We adopt the harmonic-oscillator range parameter $b \approx 1 \times A^{1/6}$ fm. We use the effective charges $e_{\text{eff}}^\pi = 1.5e$ and $e_{\text{eff}}^\nu = 0.5e$ for $B(E2)$ and the spectroscopic quadrupole moment $Q_{\text{sp}} = \sum_{\tau=\pi\nu} e_{\text{eff}}^\tau \sqrt{16\pi/5} \langle r^2 Y_{20} \rangle_\tau$, where the symbol $\langle \ \rangle$ denotes an expectation value.

III. CALCULATED RESULTS AND DISCUSSIONS

A. Positive-parity states

Calculated energy levels with positive parity are compared with the experimental ones of Ref. [16], in Fig. 1. The experimental bands are labeled with the same numbers as those used in Ref. [16], where these bands are classified according to observed electromagnetic transitions. Similarly, we classify the calculated energy levels into bands according to cascade series of large $B(E2 : J \rightarrow J-2)$ values. It should be noted that the calculated $B(E2 : J \rightarrow J-2)$ value is very small when the two states with $J-2$ and J belong to different bands. We calculated also $B(M1 : J \rightarrow J-1)$ values to compare with experimentally observed $J \rightarrow J-1$ transitions. We use the free-nucleon effective g -factors for calculations of $M1$ and $M2$ transition strengths. In the calculations, the pairs of $(13/2_1^+, 13/2_2^+)$, $(17/2_2^+, 17/2_3^+)$, and $(21/2_1^+, 21/2_2^+)$ almost degenerate in energy, respectively. We classify the $21/2_2^+$ state as the member of the band 1 from the value $B(E2 : 25/2_3^+ \rightarrow 21/2_2^+) = 12.7$ Weisskopf unit (W.u.) much larger than $B(E2 : 25/2_3^+ \rightarrow 21/2_1^+) = 0.15$ W.u. This is consistent with the calculated values $B(M1 : 23/2_1^+ \rightarrow 21/2_2^+) \gtrsim B(M1 : 23/2_1^+ \rightarrow 21/2_1^+) \sim 0.02$ W.u., $B(E2 : 23/2_1^+ \rightarrow 21/2_2^+) = 1.7$ W.u., and $B(E2 : 23/2_1^+ \rightarrow 21/2_1^+) = 0.03$ W.u. For $13/2^+$, we have the values $B(M1 : 15/2_1^+ \rightarrow 13/2_1^+) = 2.96$ W.u., $B(M1 : 15/2_1^+ \rightarrow 13/2_2^+) = 0.95$ W.u., $B(E2 : 15/2_1^+ \rightarrow 13/2_1^+) = 12.6$ W.u., and $B(E2 : 15/2_1^+ \rightarrow 13/2_2^+) = 0.70$ W.u. These values suggest that the $13/2_1^+$ state is another candidate for the $13/2^+$ state observed in the band 1, although the $B(E2)$ values for the cascade decay $17/2_3^+ \rightarrow 13/2_1^+ \rightarrow 9/2_1^+$ are smaller than those for $17/2_3^+ \rightarrow 13/2_2^+ \rightarrow 9/2_1^+$. We get calculated values $B(E2 : 11/2_1^+ \rightarrow 9/2_1^+) = 7.3$ W.u. and $B(M1 : 11/2_1^+ \rightarrow 9/2_1^+) = 0.22$ W.u. This indicates a strong $E2$ transition for $11/2_1^+ \rightarrow 9/2_1^+$.

We cannot find the $27/2^+$ ($29/2^+$) member belonging to the band 1 ($1'$) among the lowest five states with $J = 27/2$ ($J = 29/2$) in calculations. These states with $J^\pi \geq 27/2^+$ have different configurations from the states with $J^\pi \leq 23/2^+$ and the $25/2_3^+$ state as discussed later. Therefore, the $27/2^+$ and $29/2^+$ members are missing in the calculated band 1 ($1'$) in Fig. 1. Our model predicts the $25/2_4^+$ state as a member of the band 3. The calculated results thus show deviations from the experimental data [16] and suggest that mixing of wave functions should be improved. However, our model reproduces qualitatively well a lot of observed energy levels and basically explains the experimental band classifications. It is difficult to get such a good quality of agreement with experiment using other models at present. The structure study of ^{69}As with our model is worthwhile.

Let us analyze obtained wave functions and consider the structure which characterizes the observed bands.

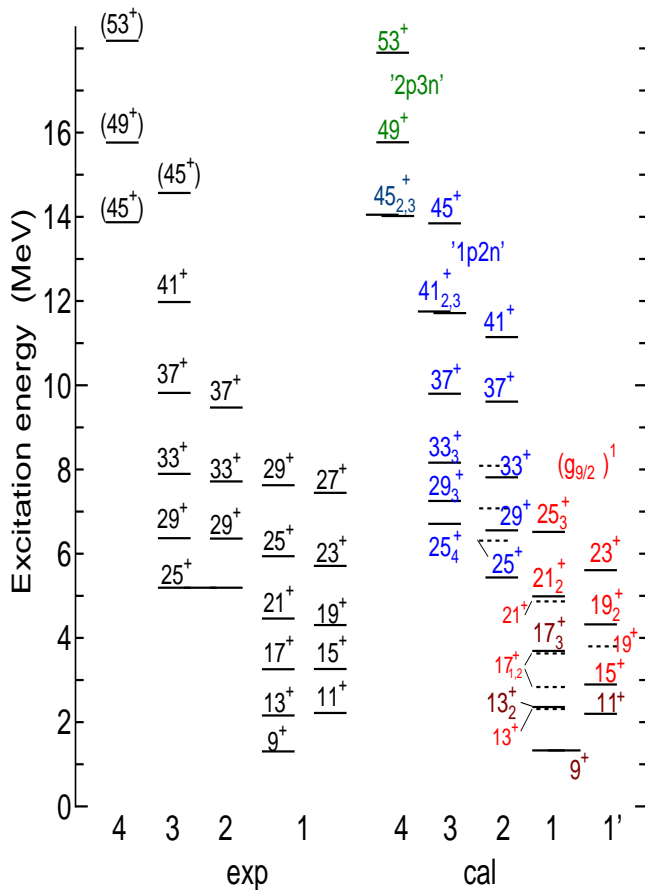


FIG. 1: Experimental and calculated energy levels with positive parity. The spin of each state is denoted by the double number $2J$. Non-yrast states are distinguished with the subscripts which represent the numerical order for each spin, while the subscript 1 is omitted for the yrast states. In addition to these “collective states”, nearby levels which have the same spin as that of the collective states are plotted using the dashed lines.

We calculated the following quantities for every state: (1) expectation values of proton and neutron numbers in the four orbits which are denoted by $\langle n_a^\pi \rangle$ and $\langle n_a^\nu \rangle$; (2) expectation values of spin and isospin in the high- j intruder orbit $g_{9/2}$ and in the pf shell ($p_{3/2}, f_{5/2}, p_{1/2}$) which are evaluated as $\langle J_i \rangle = [\langle \hat{j}_i^2 \rangle + 1/4]^{1/2} - 1/2$ and $\langle T_i \rangle = [\langle \hat{t}_i^2 \rangle + 1/4]^{1/2} - 1/2$, where \hat{j}_i and \hat{t}_i are spin and isospin operators for $i = g_{9/2}$ or $i = pf$; (3) spectroscopic quadrupole moment Q_{sp} . These quantities are useful in investigating structure change in a series of states [12, 13, 14, 15].

In Fig. 2, we illustrate the expectation values $\langle n_{g_{9/2}}^\pi \rangle$, $\langle n_{g_{9/2}}^\nu \rangle$, $\langle J_i \rangle$, and $\langle T_i \rangle$ ($i = g_{9/2}, pf$) for the positive-parity bands. Figure 2 indicates that the classifications of bands correspond to different configurations. As the spin J increases, the positive-parity states pass three stages A, B, and C classified by the occupation number $\langle n_{g_{9/2}}^\pi \rangle + \langle n_{g_{9/2}}^\nu \rangle$: [Stage A] states with $J^\pi \leq 23/2^+$ and the $25/2_3^+$ state have $\langle n_{g_{9/2}}^\pi \rangle + \langle n_{g_{9/2}}^\nu \rangle < 1.5$; [Stage B] states with $25/2^+ \leq J^\pi \leq 41/2^+$ and the $45/2_1^+$ state have $\langle n_{g_{9/2}}^\pi \rangle \approx 1$ and $\langle n_{g_{9/2}}^\nu \rangle \approx 2$; [Stage C] states with $49/2^+ \leq J^\pi \leq 53/2^+$ and the $45/2_{2,3}^+$ states have

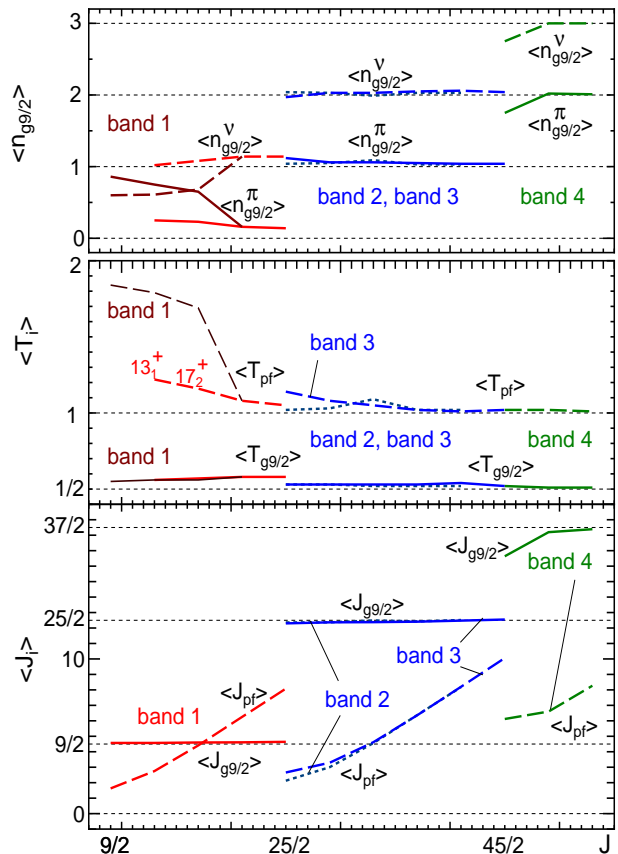


FIG. 2: The expectation values $\langle n_{g_{9/2}}^\nu \rangle$ and $\langle n_{g_{9/2}}^\pi \rangle$ in the upper panel, and the expectation values $\langle T_i \rangle$ and $\langle J_i \rangle$ ($i = g_{9/2}, pf$) in the lower panel, for the positive-parity bands.

$\langle n_{g_{9/2}}^\pi \rangle \approx 2$ and $\langle n_{g_{9/2}}^\nu \rangle \approx 3$. (Note that a basis state with positive parity has an odd number of $g_{9/2}$ nucleons.) The band 1 is at the stage A (which is composed of two series of the favored states with $J = 9/2 + 2l$ ($\alpha = 9/2$) and unfavored states with $J = 7/2 + 2l$ ($\alpha = 9/2 - 1$), where l being an integer), the bands 2 and 3 are at the stage B, and the band 4 is at the stage C. These results for the bands 2, 3, and 4 are consistent with the results of cranked Nilsson-Strutinsky calculations in Ref. [16]. The lower panel of Fig. 2 displays angular momentum alignments. In the bands 2 and 3, one proton and two neutrons ($1p2n$) in the $g_{9/2}$ orbit align their spins to be $\langle J_{g_{9/2}} \rangle \approx 25/2$ ($9/2 + 9/2 + 7/2$) and fold their isospins to be minimum $\langle T_{g_{9/2}} \rangle \approx 1/2$. In the band 4, two protons and three neutrons ($2p3n$) in the $g_{9/2}$ orbit align their spins to be $\langle J_{g_{9/2}} \rangle \approx 37/2$ and fold their isospins to be $\langle T_{g_{9/2}} \rangle \approx 1/2$. Thus, the experimental bands 2 and 3 are the $1p2n$ aligned bands and the band 4 is the $2p3n$ aligned band.

The structure of the lowest positive-parity band 1 was not much discussed in Ref. [16]. Our calculations reveal unique structure in these states. According to the ENSDF data [22], the lowest positive-parity state $9/2_1^+$ has a long life-time $t_{1/2} = 1.35(4)$ ns, which reminds us about the isomeric state $9/2_1^+$ of ^{67}As ($t_{1/2} = 12(2)$ ns). For the $9/2_1^+$ state of ^{69}As , we obtain the expectation values $\langle n_{g_{9/2}}^\pi \rangle = 0.86$, $\langle n_{g_{9/2}}^\nu \rangle = 0.60$, $\langle J_{g_{9/2}} \rangle \approx 9/2$, and $\langle T_{g_{9/2}} \rangle \approx 1/2$ which are similar to those of the $9/2_1^+$ state in ^{67}As (see Ref. [15]). This result suggests that the $9/2_1^+$ state is not simply expressed as $(g_{9/2}^\pi) \otimes ^{68}\text{Ge}$ but has a significant component of $(g_{9/2}^\nu) \otimes ^{68}\text{As}$, indicating that one neutron competes with one proton for jumping in the high- j orbit $g_{9/2}$ in this odd-proton nucleus. The unique structure of the $9/2_1^+$ state retards $E3$ and $M2$ transitions to the lower negative-parity states, *i.e.*, $B(E3 : 9/2_1^+ \rightarrow 3/2^-, 5/2^-, 7/2^-) < 0.08$ and $B(M2 : 9/2_1^+ \rightarrow 5/2^-, 7/2^-) < 0.38$ in W.u., because the negative-parity states with $J^\pi \leq 7/2^-$ below the $9/2_1^+$ state are collective states strongly mixed in the pf space as discussed later. The $5/2^+$ and $7/2^+$ states are above the $9/2_1^+$ state in our results. Our model is thus consistent with the long-life property of the $9/2_1^+$ state in ^{69}As as in ^{67}As [15]. The states $13/2_2^+$ and $17/2_3^+$ have large neutron occupation numbers $\langle n_{g_{9/2}}^\nu \rangle = 0.61$ and $\langle n_{g_{9/2}}^\nu \rangle = 0.68$, respectively. They have structure similar to the $9/2_1^+$ state and are possibly members of the band 1 on $9/2_1^+$. We note here that calculated Q_{sp} values are negative (prolate) for positive-parity states.

The trend that a neutron is apt to jump in the $g_{9/2}$ orbit manifests itself clearly in other states with $11/2^+ \leq J^\pi \leq 23/2^+$ and in the $25/2_3^+$ state. These states have one neutron instead of one proton in the $g_{9/2}$ orbit (see Fig. 2) and can be called “high- j $1n$ ” states. We can say that the backbending from $21/2_1^+$ to $25/2_1^+$ in ^{69}As is caused by the “ $1p1n$ alignment” in contrast to the discussion in Ref. [10]. This is unexpected structure in

odd-proton nuclei. The results suggest that the residual $A = 68$ system excluding one $g_{9/2}$ nucleon favors an odd-odd subsystem with $T_{pf} = 1$ analogous to ^{68}As rather than an even-even subsystem with $T_{pf} = 2$ analogous to ^{68}Ge . Because there is no energy difference between $1p$ and $1n$ in the $g_{9/2}$ orbit, the $A = 68$ subsystems with $T_{pf} = 2$ and $T_{pf} = 1$ compete with each other. It should be noted here that the $T = 0$ monopole field $H_{\pi\nu}^{T=0}$, which brings about the bulk of the symmetry energy depending on the total isospin [23], does not have any effect on the subsystem but operates on the total isospin of the whole system. The $A = 68$ subsystem with $\langle J_{pf} \rangle \approx 0$ and $\langle T_{pf} \rangle \approx 2$ is probably superior in energy for the $9/2_1^+$ state. For the $J^\pi > 9/2^+$ states excluding $13/2_2^+$ and $17/2_3^+$, however, the $A = 68$ subsystem with $T_{pf} \approx 1$ can increase angular momentum with less energy. This is the reason why the yrast states with $11/2^+ \leq J^\pi \leq 23/2^+$ have mainly one neutron in the $g_{9/2}$ orbit, in our shell model. The same mechanism probably produces such “high- j $1n$ ” states in odd-proton $N \approx Z$ nuclei.

Our calculations predict another configuration for the yrast states $35/2_1^+$, $39/2_1^+$, and $43/2_1^+$. These states have the expectation values $\langle n_{g_{9/2}}^\pi \rangle = 1.7 \sim 1.5$, $\langle n_{g_{9/2}}^\nu \rangle = 1.4 \sim 1.6$, $\langle J_{g_{9/2}} \rangle \approx 25/2$, and $\langle T_{g_{9/2}} \rangle \approx 1/2$, which suggests that these yrast states are mixed states of the $2p1n$ and $1p2n$ aligned states. It is interesting that the $2p1n$ alignment contributes significantly to the unfavored states with $J^\pi = (7/2 + 2l)^+$. No detection of the $J^\pi = (7/2 + 2l)^+$ (unfavored) band at spins $J^\pi \geq 31/2^+$ in experiment [16] seems to be related to the mixed structure of the $J^\pi = (7/2 + 2l)^+$ band different from the $J^\pi = (9/2 + 2l)^+$ (favored) band.

B. Negative-parity states

Let us turn our attention to negative-parity states. Calculated negative-parity energy levels are compared with the experimental ones [16] in Fig. 3, where the experimental bands are labeled with the same numbers as those used in Ref. [16] and corresponding theoretical bands are classified according to cascade series of large $B(E2 : J \rightarrow J - 2)$ values. The calculated level scheme shows quantitative deviations from the experimental one [16] in some details. The deviations suggest adjusting finely the parameters of the model Hamiltonian or introducing effects excluded from it. However, a lot of experimental energy levels are qualitatively well reproduced except that the calculation lays the collective states ($3/2_1^-$ and $5/2_1^-$) and ($15/2_2^-$ and $19/2_1^-$) in reverse order. The calculated four bands are basically in agreement with the experimental ones.

Our shell model shows that, in a parallel manner to the positive-parity states, each of the negative-parity bands can be divided into three stages A, B, and C: The occupation number in the $g_{9/2}$ orbit is $\langle n_{g_{9/2}}^\pi \rangle + \langle n_{g_{9/2}}^\nu \rangle < 0.57$ at the stage A, $\langle n_{g_{9/2}}^\pi \rangle + \langle n_{g_{9/2}}^\nu \rangle \sim 2$ at the stage B, and

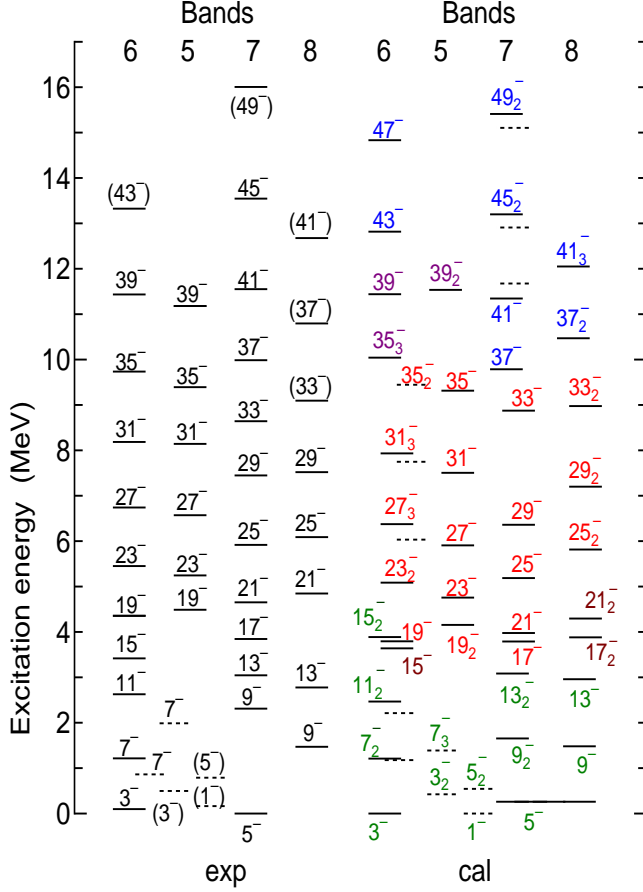


FIG. 3: Experimental and calculated energy levels with negative parity, illustrated in the same manner as Fig. 1.

$\langle n_{g9/2}^{\pi} \rangle + \langle n_{g9/2}^{\nu} \rangle \sim 4$ at the stage C. (Note that a basis state with negative parity has an even number of $g_{9/2}$ nucleons.) The three stages of each band are distinguished by illustrating them at somewhat shifted columns in Fig. 3. In Fig. 4, by way of example, we illustrate how the bands 7 and 8 change the expectation values $\langle n_{g9/2} \rangle$ and $\langle J_{g9/2} \rangle$ at the three stages. It is reasonable to separate a negative-parity band into the three sub-bands from the parallelism between Figs. 1 (2) and 3 (4). Let us call the three sub-bands, for instance, 7A, 7B, and 7C.

The low-spin states with $J^{\pi} \leq 7/2^{-}$ below $9/2_1^{+}$ have only fractional numbers of nucleons in the $g_{9/2}$ orbit, $\langle n_{g9/2}^{\pi} \rangle < 0.20$ and $\langle n_{g9/2}^{\nu} \rangle < 0.33$. The occupation numbers in the three orbits ($p_{3/2}, f_{5/2}, p_{1/2}$) show that these low-spin states are collective states strongly mixed in the pf space. This is in disagreement with the conjecture in Ref. [16] that the low-lying negative-parity states have single-particle character. Our model lays the collective state $3/2_1^{-}$ slightly below the $5/2_1^{-}$ state for the odd-proton $N \approx Z$ nuclei ^{69}As and ^{67}As [15], which is inconsistent with the experimental ground state $5/2_1^{-}$. However, our model reproduces the correct ground states $3/2_1^{-}$ and $1/2_1^{-}$ respectively for the odd-neutron $N \approx Z$

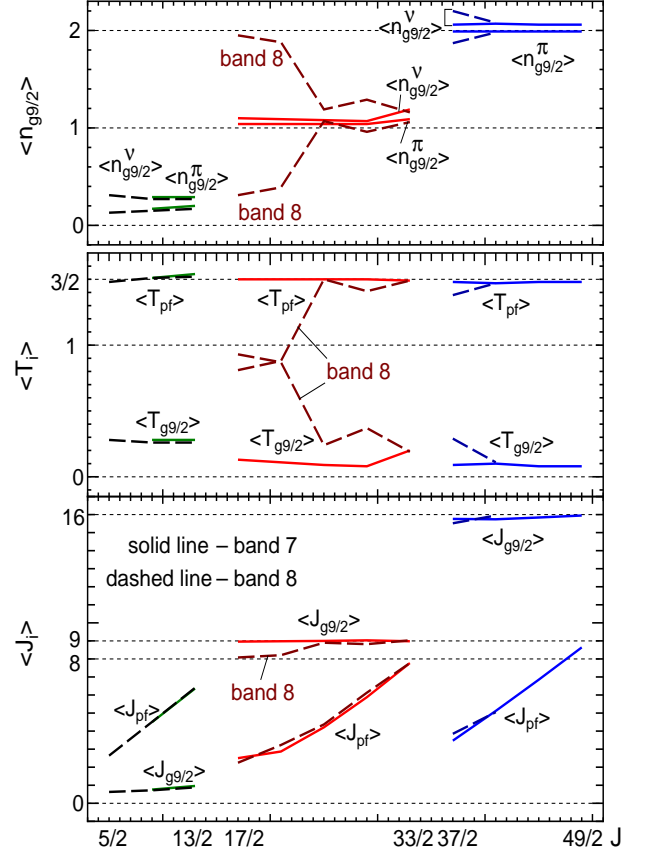


FIG. 4: The expectation values $\langle n_{g9/2}^{\nu} \rangle$, $\langle n_{g9/2}^{\pi} \rangle$, $\langle T_i \rangle$, and $\langle J_i \rangle$ ($i = g_{9/2}, pf$) for the negative-parity bands 7 and 8.

nuclei ^{65}Ge and ^{67}Ge [14]. In Fig. 3, tentatively assigned $1/2_1^{-}$, $3/2_2^{-}$, and $5/2_2^{-}$ states [22] are considerably well reproduced with our model. Repeated calculations by changing the parameters within the extended $P+QQ$ Hamiltonian have not succeeded to get a $5/2_1^{-}$ ground state in odd-mass As isotopes. The reversed order of $5/2_1^{-}$ and $3/2_1^{-}$ suggests an effect missing in our model. There is a possibility that the imposed isospin symmetry is too severe for reproducing different ground states in the $N = 33$ nucleus ^{65}Ge and the $Z = 33$ nuclei (^{67}As , ^{69}As).

It is interesting that in calculated results the lowest sub-bands 6A ($3/2_1^{-}, 7/2_2^{-}, 11/2_2^{-}, 15/2_2^{-}$) and 8A ($5/2_1^{-}, 9/2_1^{-}, 13/2_1^{-}$) have distinctly positive and negative signs of spectroscopic quadrupole moments Q_{sp} as shown in Table I. The shell model calculations using the present

TABLE I: Calculated spectroscopic quadrupole moments Q_{sp} in $e \text{ fm}^2$ for the lowest two sub-bands 6A and 8A.

6A	$3/2_1^{-}$	$7/2_2^{-}$	$11/2_2^{-}$	$15/2_2^{-}$
Q_{sp}	22	18	41	13
8A	$5/2_1^{-}$	$9/2_1^{-}$	$13/2_1^{-}$	
Q_{sp}	-30	-19	-17	

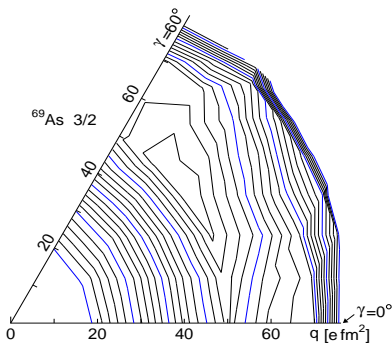


FIG. 5: The energy surface $\langle q, \gamma | H | q, \gamma \rangle$ in the $q - \gamma$ plane ($0^\circ \leq \gamma \leq 60^\circ$) plotted with contours.

model [12, 13, 14, 15] give \pm signs of Q_{sp} to the 2_1^+ and 2_2^+ states in even-even Zn and Ge isotopes with $N \approx Z$ and to the 1_1^+ and 3_1^+ states in ^{66}As , but do not produce distinct two bands with $Q_{sp} = \pm$ for these nuclei. Only for ^{68}Se , in our calculations, we got oblate-prolate shape coexistence as two bands with $Q_{sp} = \pm$. (That is confirmed by the two minima of the potential energy surface drawn in the $q - \gamma$ plane in the constrained HF calculation for the same Hamiltonian [13].) Therefore, the coexistence of the two bands with $Q_{sp} = \pm$ in an odd-mass $N \approx Z$ nucleus is remarkable. It is known, however, that in this mass region the potential energy mostly has minima both in prolate and oblate shapes under the condition of axial symmetry. In order to determine the shapes of the pair of $Q_{sp} = \pm$ bands, we must examine the potential energy surface in the $q - \gamma$ plane. We carried out the constrained HF calculation [24, 25] for ^{69}As . The result is illustrated in Fig. 5, where q is the intrinsic quadrupole moment (the unit is efm^2). We have the relation $Q_{sp} \propto q(e_\pi + e_\nu)/e$ but cannot easily express its coefficient in the triaxial situation shown in Fig. 5. This figure shows that in low energy ^{69}As favors a triaxial shape in the $q - \gamma$ plane but the shallow and broad minimum indicates rather γ -unstable nature. Thus, the coexistence of the $Q_{sp} = \pm$ bands in ^{69}As is different from the oblate-prolate shape coexistence in ^{68}Se but is a unique phenomenon in an odd-mass nucleus. The last odd nucleon must play an important role in kinematically determining the nuclear shape. The two angular momentum couplings $J = 5/2 + 2l$ (favored) and $J = 3/2 + 2l$ (unfavored) seem to have different effects on Q_{sp} .

For high-spin negative-parity states, only $2n$, $1p3n$, and $2p2n$ configurations in the $g_{9/2}$ orbit are considered in Ref. [16]. In contrast Fig. 4 displays that unexpected structure appears in the sub-bands 7B and 8B with $17/2^- \leq J^\pi \leq 33/2^-$. The present shell model predicts the $1p1n$ configuration in the $g_{9/2}$ orbit ($\langle n_{g_{9/2}}^\pi \rangle \approx 1$ and $\langle n_{g_{9/2}}^\nu \rangle \approx 1$) for the states of the sub-bands 7B and 8B (also for the states of the sub-bands 5B and 6B with $19/2^- \leq J^\pi \leq 35/2^-$) except for the states $17/2_2^-$ and $21/2_2^-$. The $1p1n$ pair in the $g_{9/2}$ orbit has $\langle T_{g_{9/2}} \rangle \approx 0$ and $\langle J_{g_{9/2}} \rangle \approx 9$ as shown in the lower panel of Fig. 4,

which indicates the $T = 0$, $J = 9$ $1p1n$ alignment in the high- j orbit $g_{9/2}$. The shell model calculations have already shown the same $1p1n$ alignment in even-even and odd-odd $N \approx Z$ nuclei (^{62}Zn , $^{64-68}\text{Ge}$, ^{68}Se , and ^{66}As) [12, 14, 15]. Therefore we can say that the $T = 0$, $J = 9$ $1p1n$ alignment is a general phenomenon in $N \approx Z$ nuclei of this mass region. We can expect the same structure also in ^{72}Kr , ^{72}Br , ^{73}Br , etc.

When the $T = 0$, $J = 9$ $1p1n$ alignment takes place in ^{69}As , the residual $A = 67$ subsystem excluding the $g_{9/2}$ nucleons has the isospin $T_{pf} = 3/2$ analogous to ^{67}Ge (see Fig. 4). The $T = 0$ $1p1n$ alignment is not only due to a large energy gain of the $T = 0$, $J = 9$ $1p1n$ pair in the $g_{9/2}$ orbit but also due to low energy of the residual $A = 67$ subsystem. The competition between the $A = 67$ subsystems with $T_{pf} = 3/2$ and $T_{pf} = 1/2$ affects the competition between the $T = 0$ $1p1n$ alignment and $T = 1$ $2n$ alignment in the $g_{9/2}$ orbit. In our calculations, the $2n$ aligned state $17/2_2^-$ ($21/2_2^-$) is higher in energy than the $1p1n$ aligned state $17/2_1^-$ ($21/2_1^-$), and the $2n$ aligned state does not appear in the lowest two states of each J when $23/2^- \leq J^\pi \leq 35/2^-$. This situation possibly explains the reason why the experiment [16] detected only one $17/2^-$ state in the doublet of $J^\pi = (5/2 + 2l)^-$ bands. The results $\langle n_{g_{9/2}}^\pi \rangle \approx 0.67$ and $\langle n_{g_{9/2}}^\nu \rangle \approx 1.57$ for $15/2_1^-$ suggest that the $15/2_1^-$ state is a mixture of the $1p1n$ and $2n$ aligned states.

In our calculations, the $J^\pi \geq 37/2^-$ states have the aligned $2p2n$ in the $g_{9/2}$ orbit except that the states $39/2_1^-$ and $39/2_2^-$ have mixed components of the aligned $1p3n$. This is consistent with the result of cranked Nilsson-Strutinsky calculations in Ref. [16]. The calculated $35/2_3^-$ state is the $2p2n$ aligned state mixed with the $1p3n$ aligned state and is a candidate for the $35/2^-$ member of the band 6.

IV. CONCLUSION

The analysis of ^{69}As by means of large-scale shell model calculations has revealed unexpected features of structure. In this odd-proton $N \approx Z$ nucleus in which the high- j intruder orbit $g_{9/2}$ plays an important role, one neutron competes with one proton for occupying the $g_{9/2}$ orbit in the states $9/2_1^+$, $13/2_2^+$, and $17/2_3^+$. Moreover, one neutron almost solely occupies the $g_{9/2}$ orbit in other positive-parity states with $J^\pi \leq 23/2^+$. This trend makes higher-spin states be the $1p2n$ and $2p3n$ aligned states. For the negative-parity states, the present shell model indicates the $T = 0$, $J = 9$ $1p1n$ alignment in the $g_{9/2}$ orbit, in an odd-mass nucleus as well as odd-odd and even-even nuclei. These unique configurations take place in cooperation with the characteristic that the $N \approx Z$ subsystems with different T excluding the $g_{9/2}$ nucleons nearly degenerate in energy. The present model also predicts the coexistence of two lowest bands with $Q_{sp} = \pm$ different from the known oblate-prolate shape

coexistence, in the odd-mass nucleus ^{69}As . This work and a series of our papers [12, 13, 14, 15] clarified a vari-

ety of interesting phenomena in $N \approx Z$ nuclei, providing a useful perspective for studying neighboring nuclei.

-
- [1] S. M. Fischer *et al.*, Phys. Rev. Lett. **87**, 132501 (2001).
 [2] E. Bouchez *et al.*, Phys. Rev. Lett. **90**, 082502 (2003).
 [3] S. M. Fischer, C. J. Lister, D. P. Balamuth, Phys. Rev. C **67**, 064318 (2003).
 [4] E. A. Stefanova *et al.*, Phys. Rev. C **67**, 054319 (2003).
 [5] P. Sarriguren, E. Moya de Guerra, and A. Escuderos, Nucl. Phys. **A658**, 13 (1999).
 [6] A. Petrovici, K. W. Schmid, and A. Faessler, Nucl. Phys. **A710**, 246 (2002).
 [7] M. Kobayashi, T. Nakatsukasa, M. Matsuo, and K. Matsuyanagi, Prog. Theor. Phys. **110**, 65 (2003); nucl-th/0412062.
 [8] Y. Sun, Eur. Phys. J. A **20**, 133 (2004).
 [9] D. Alehed and N. R. Walet, nucl-th/0406028.
 [10] A. M. Bruce *et al.*, Phys. Rev. C **62**, 027303 (2000).
 [11] D. G. Jenkins *et al.*, Phys. Rev. C **64**, 064311 (2001).
 [12] M. Hasegawa, K. Kaneko, and T. Mizusaki, Phys. Rev. C **70**, 031301(R) (2004).
 [13] K. Kaneko, M. Hasegawa, and T. Mizusaki, Phys. Rev. C **70**, 051301(R) (2004).
 [14] M. Hasegawa, K. Kaneko, and T. Mizusaki, Phys. Rev. C **71**, 044301 (2005).
 [15] M. Hasegawa, Y. Sun, K. Kaneko, and T. Mizusaki, Phys. Lett. B **617**, 150 (2005).
 [16] I. Stefanescu, J. Eberth, G. Gersch, T. Steinhardt, O. Thelen, N. Warr, D. Weisshaar, B. G. Carlsson, I. Ragnarsson, G. de Angelis, T. Martinez, A. Jungclaus, R. Schwengner, K. P. Lieb, E. A. Stefanova, and D. Curien, Phys. Rev. C **70**, 044304 (2004).
 [17] D. Rudolph *et al.*, Eur. Phys. J. A **6**, 377 (1999).
 [18] A. Juodagalvis and S. Åberg, Nucl. Phys. **A683**, 206(2001).
 [19] T. Mizusaki, RIKEN Accel. Prog. Rep. **33**, 14 (2000).
 [20] T. Mizusaki and M. Imada, Phys. Rev. C **65**, 064319 (2002); **67**, 041301(R) (2003).
 [21] T. Mizusaki, in press.
 [22] <http://www.nndc.bnl.gov/nndc/ensdf>
 [23] K. Kaneko and M. Hasegawa, Phys. Rev. C **69**, 061302(R) (2004); Prog. Theor. Phys. **106**, 1179 (2001).
 [24] T. Mizusaki, T. Otsuka, Y. Utsuno, M. Honma, and T. Sebe, Phys. Rev. C **59**, R1846 (1999).
 [25] K. Hara, Yang Sun, and T. Mizusaki, Phys. Rev. Lett. **83**, 1922 (1999).